

Proposed measurement of coherence and phase sensitivity in a mesoscopic system

Gang Zhang,^{1,2,*} Zhiliang Cao,¹ Wenhui Duan,² and Bing-Lin Gu^{1,2}

¹Center for Advanced Study, Tsinghua University, Beijing 100084, People's Republic of China

²Department of Physics, Tsinghua University, Beijing 100084, People's Republic of China

(Received 12 July 2000; revised manuscript received 2 November 2000; published 23 March 2001)

We study the transport through a mesoscopic system that consists of an Aharonov-Bohm ring and a quantum dot. The ring, with the quantum dot embedded in one of its arms, is connected to a normal conductor and a superconductor. In such a system with a superconductor, holes are introduced due to the Andreev reflection at the normal-conductor–superconductor interface, and contribute to the total transport current. Using the waveguide theory, we find that holes do not influence the phase characteristic of the total transport current, but they do influence the magnitude of the current. A significant dependence of the transport current on the length of the lead that connects the ring to the superconductor is observed.

DOI: 10.1103/PhysRevB.63.155302

PACS number(s): 73.23.Hk, 85.35.Ds, 85.25.-j

Quantum interference effects have been observed in mesoscopic systems where the wave nature of electrons plays an important role. To fully characterize the transport properties of electrons through such systems, phase evolution information must be provided. It has been suggested that the phase can be measured in some interference systems. Recently, the phase behaviors of electrons traversing a quantum dot (QD) were studied both experimentally and theoretically.^{1–5} It was pointed out that the small size of mesoscopic systems induces Coulomb blockade effects and it is necessary to generalize the Landauer-Büttiker formalism to these systems. In 1995, Yacoby *et al.* measured the transmission phase through a QD, and directly demonstrated that phase coherent transport through quantum dots in realistic systems may not be destroyed by inelastic scattering.¹ Two distinguishing features were observed in this experiment: first, the phase of Aharonov-Bohm (AB) oscillations changes abruptly when the conductance of the AB ring passes a peak; second, the AB oscillations at consecutive conductance peaks are in phase. The abrupt phase change at resonance can be understood because the conductance should be an even function of the external magnetic field.^{6,7} Some other authors, however, argued that it might result from the electron-electron interaction. Using a self-consistent mean-field approximation to treat the electron-electron interaction within the QD and considering several channels in the AB ring, they also got the result of a sudden phase change by π in the oscillations.^{8,9} It is more difficult to understand the second feature of in-phase behavior observed by Yacoby *et al.*¹ since neither integrable nor chaotic quantum dots were expected to have the same phase between successive resonances. Considering both the resonance of the dot and the interference effect, Wu *et al.* explained the in-phase behavior¹⁰ in a one-dimensional noninteracting model. For two-terminal structures, it is almost impossible to measure the transmission phase of the quantum dot because of the phase rigidity enforced by the transmission coefficient.¹¹ Schuster and Buks¹² measured the transmission phase of a quantum dot in a modified four-terminal geometry where the phase rigidity does not apply. They observed continuous phase shifts of the AB oscillations as a function of the gate voltage on the quantum dot. More recently, Ferrari *et al.*⁵

found that the persistent current through a quantum dot embedded in a mesoscopic ring in the Kondo regime is enhanced relative to the current in a perfect ring of the same length, and depends only on the states in the vicinity of the Fermi level.

In order to provide comprehensive information about electron transport in mesoscopic systems, in this paper, we propose a different structure and focus our study on it. This structure consists of an AB ring and a QD, and, with two leads, is connected to a normal conductor and a *superconductor* [as shown in Fig. 1(a)]. When a normal conductor is placed near a superconductor, the electronic properties of the normal conductor can be affected by the nearby superconductor. This is the superconducting proximity effect. When an electron in the normal conductor moves to the interface between the normal conductor and the superconductor (NS),

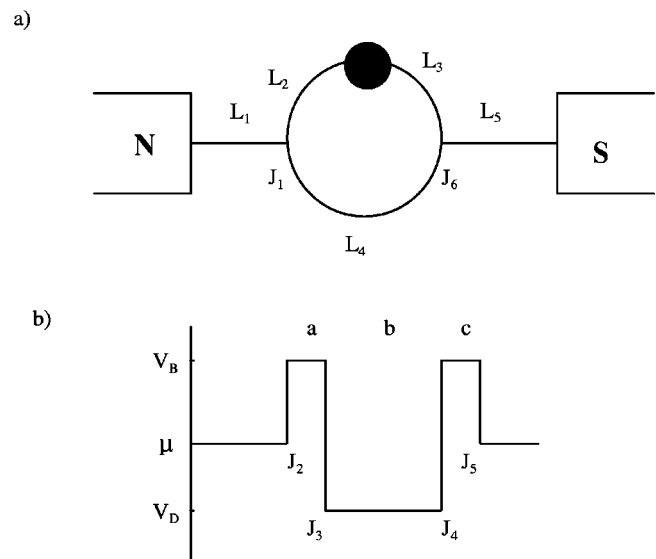


FIG. 1. (a) The mesoscopic system we study. A QD is embedded in an AB ring with two leads. This ring is connected to a normal metal and a superconductor. (b) The on-site energies for the system. The widths of the barrier and the well are W_1 and W_2 , respectively. The effective electrostatic potential of the arm with the dot is parametrized by V_D (dot potential) and V_B (barrier potential).

Andreev reflection occurs.¹³ In this case, a Cooper pair goes into the superconductor and then a hole reflects back. So the current in the normal conductor has two parts: the contribution from the electrons and that from the holes. In 1982, Blonder, Tinkham, and Klapwijk^{14–16} studied the superconducting proximity effect. They assumed a repulsive potential $[H\delta(x)]$ located at the interface and got the reflection coefficients of holes and electrons via Andreev reflection when electrons are reflected at the NS interface by solving the Bogoliubov equations. As we know, electrons and holes have different wave vectors and different additional phases under a magnetic field. Hence the coherence and phase sensitivity in such a mesoscopic system can be very different compared with the usual systems without a superconductor. Since the single-channel model provides a good approximation to a real wire with finite width at low temperature, we restrict our model to the one-channel case. In this paper, we investigate the effects of quantum interference on the transport current in the structure by use of one-dimensional waveguide theory.

In a mesoscopic system, the transport properties are very sensitive to the size of the system. When the size is comparable with or less than the characteristic lengths, i.e., the phase-breaking length $L_\phi = (D\tau_\phi)^{1/2}$ and the coherence length $L_T = (\hbar D/k_B T)^{1/2}$ (τ_ϕ is the sum of the scattering rates when the phase of an electron is disrupted, and D is the electron diffusion constant), the electron maintains phase memory throughout the system. L_ϕ and L_T are of the order of 0.1–2 μm in metallic thin film at liquid-helium temperature. It is important to discuss the hole lifetime in our system before we study the coherence characteristics of holes. The quasiparticle lifetime in metals has been investigated by use of the free-electron gas (FEG) model of the Fermi liquid. In this simple model, for either electrons or holes with energy E very near the Fermi level E_F , the inelastic lifetime is found to be proportional to $(E - E_F)^{-2}$.¹⁷ First principles calculations^{18,19} for particle lifetimes in noble metals have been carried out only very recently, and indicate that both electrons and holes exhibit lifetimes well over those predicted within the FEG model, due to a major contribution from the occupied d states participating in the screening of the electron-electron interactions. It was found that the lifetime of holes in copper is on the order of 10^2 fs while $|E - E_F| \sim 1$ eV.¹⁹ Obviously, a much larger hole lifetime can be expected for energies near the Fermi level. The Fermi velocity in copper is about 1.6×10^8 cm/s.²⁰ Thus the mean free path of holes in copper can be much larger than 0.16 μm . In fact, according to conventional proximity effect theory, the Cooper pair amplitude decays exponentially with distance into a normal metal having electron diffusion constant larger than the characteristic length, and under these conditions holes as well as electrons retain phase memory as they diffuse inside the normal wire.²¹ It should be possible to fabricate our proposed mesoscopic structure by means of multilayer lithography with a submicrometer precision of the alignment. In this structure, the transport current is significantly affected by Andreev reflection, which introduces holes into the system, and both electrons and holes contribute to the current.

Figure 1(b) shows the on-site energies of the system. The chemical potential outside the dot is referred to as μ . The effective electrostatic potential in the arm with the dot is parametrized by the quantities V_D (dot potential) and V_B (barrier potential). The normal-conductor–superconductor junction leads to a δ -function potential with strength Z_0 . We follow the method used in our previous work to calculate the transport current.²² In the local coordinate system, the wave functions in the circuit [as shown in Fig. 1(a)] can be given as follows:

$$\begin{aligned} \Psi_1(x_1) &= \begin{pmatrix} 1 \\ 0 \end{pmatrix} e^{ik_e x_1} + R_1^e \begin{pmatrix} 1 \\ 0 \end{pmatrix} e^{-ik_e x_1} + R_1^h \begin{pmatrix} 0 \\ 1 \end{pmatrix} e^{ik_h x_1}, \\ \Psi_i(x_i) &= A_i^e \begin{pmatrix} 1 \\ 0 \end{pmatrix} e^{ik_e^+ x_i} + B_i^e \begin{pmatrix} 1 \\ 0 \end{pmatrix} e^{-ik_e^- x_i} + A_i^h \begin{pmatrix} 0 \\ 1 \end{pmatrix} e^{-ik_h^+ x_i} \\ &\quad + B_i^h \begin{pmatrix} 0 \\ 1 \end{pmatrix} e^{ik_h^- x_i} \quad (i=2,3,4), \end{aligned} \quad (1)$$

$$\begin{aligned} \Psi_i(x_i) &= A_i^e \begin{pmatrix} 1 \\ 0 \end{pmatrix} e^{ik_{ie}^+ x_i} + B_i^e \begin{pmatrix} 1 \\ 0 \end{pmatrix} e^{-ik_{ie}^- x_i} + A_i^h \begin{pmatrix} 0 \\ 1 \end{pmatrix} e^{-ik_{ih}^+ x_i} \\ &\quad + B_i^h \begin{pmatrix} 0 \\ 1 \end{pmatrix} e^{ik_{ih}^- x_i} \quad (i=a,b,c), \end{aligned}$$

$$\begin{aligned} \Psi_5(x_5) &= A_5^e \begin{pmatrix} 1 \\ 0 \end{pmatrix} e^{ik_e x_5} + A_5^e b^e \begin{pmatrix} 1 \\ 0 \end{pmatrix} e^{-ik_e x_5} + A_5^e a^e \begin{pmatrix} 0 \\ 1 \end{pmatrix} e^{ik_h x_5} \\ &\quad + A_5^h \begin{pmatrix} 0 \\ 1 \end{pmatrix} e^{-ik_h x_5} + A_5^h b^h \begin{pmatrix} 0 \\ 1 \end{pmatrix} e^{ik_h x_5} \\ &\quad + A_5^h a^h \begin{pmatrix} 1 \\ 0 \end{pmatrix} e^{-ik_e x_5}, \end{aligned}$$

with

$$k_e = \sqrt{2m(\mu + E)}/\hbar,$$

$$k_{ie} = \sqrt{2m(\mu + E - V_B)}/\hbar \quad (i=a,c),$$

$$k_{be} = \sqrt{2m(\mu + E + V_D)}/\hbar,$$

$$k_e^\pm = k_e \pm 2\pi\phi/L\phi_0,$$

$$k_{ie}^\pm = k_{ie} \pm 2\pi\phi/L\phi_0,$$

and

$$k_h = \sqrt{2m(\mu - E)}/\hbar,$$

$$k_{ih} = \sqrt{2m(\mu - E - V_B)}/\hbar \quad (i=a,c),$$

$$k_{bh} = \sqrt{2m(\mu - E + V_D)}/\hbar,$$

$$k_h^\pm = k_h \mp 2\pi\phi/L\phi_0,$$

$$k_{ih}^\pm = k_{ih} \mp 2\pi\phi/L\phi_0,$$

where m and E are, respectively, the mass and energy of the incident electron; $k_e(k_h)$ and $k_{ie}(k_{ih})(i=a,b,c)$ are the wave vectors of electrons (holes) in the ring, well, and barrier; $k_e^\pm, k_{ie}^\pm, k_h^\pm$, and $k_{ih}^\pm (i=a,b,c)$ are the equivalent wave vectors when a magnetic flux ϕ threads the loop and destroys the time-reversal symmetry;²³ $\phi_0 (=hc/e)$ is the elementary flux quantum; and L is the circumference of the ring. Here we have introduced two-component wave functions to describe electron and hole states.

$$\begin{pmatrix} 1 \\ 0 \end{pmatrix}$$

and

$$\begin{pmatrix} 0 \\ 1 \end{pmatrix}$$

represent, respectively, the pure electron state and the pure hole state. $R_1^e (R_1^h)$ and $A_5^e (A_5^h)$ are, respectively, the reflection coefficient of electrons (holes) that are reflected back to the left reservoir and the transmission coefficient of electrons (holes) that transmit to the right. A_i^e, B_i^e, A_i^h , and $B_i^h (i=2,3,4 \text{ and } a,b,c)$ are the amplitudes of all partial waves in the loop. All coefficients can be determined by the continuity of the wave functions and the conservation of the current density at six junctions $J_i(i=1 \text{ to } 6)$ [as shown in Fig. 1(a)]. a^e and b^e are the reflection coefficients of holes and electrons via Andreev reflection when electrons are reflected at the NS interface; a^h and b^h are those of electrons and holes when holes are reflected at the NS interface. Using the method that Blonder *et al.*¹⁴ used to study Andreev reflection, we can obtain

$$a^e \approx \frac{4u_0v_0}{\Gamma}, \quad (2)$$

$$b^e \approx -\frac{Z(Z+2i)(u_0^2-v_0^2)}{\Gamma}, \quad (3)$$

$$a^h \approx \frac{4u_0v_0}{\Gamma}, \quad (4)$$

$$b^h \approx -\frac{Z(Z-2i)(u_0^2-v_0^2)}{\Gamma}, \quad (5)$$

where

$$\Gamma \equiv 4u_0^2 + Z^2(u_0^2 - v_0^2), \quad (6)$$

and Z is the dimensionless barrier strength and equal to $2Z_0/\hbar v_F$ (v_F is the Fermi velocity). u_0 and v_0 are obtained by solving the Bogoliubov equations, $u_0^2 = 1 - v_0^2 = (1 + \sqrt{E^2 - \Delta^2}/E)/2$. Here Δ is the energy gap of the superconductor. Finally, we obtain a linear 28-equation group and solve it numerically. The transport currents contributed by electrons and holes are, respectively,

$$I_e = \frac{e\hbar k_e}{m} (|A_5^e|^2 - |A_5^e b^e + A_5^h a^h|^2) \quad (7)$$

and

$$I_h = \frac{e\hbar k_h}{m} (|A_5^h|^2 - |A_5^e a^e + A_5^h b^h|^2). \quad (8)$$

The total transport currents is

$$I_T = I_e - I_h. \quad (9)$$

In our calculation, we neglect the effects of impurities, disorder, weak localization, and temperature. In the usual superconductor, the energy gap Δ is about several meV. The chemical potential μ is about 10 meV, and V_B and V_D are on the order of eV. In this paper, we select the superconductor energy gap Δ as the energy unit, the width of the barrier (W_1) as the length unit, and $e\hbar/m$ as the current unit. Then, V_B is taken to be 1000, and the width of the well (W_2) is taken to be 200. In the experiment by Yacoby *et al.*,¹ the dot size is about 0.5 μm . Our selections of parameters are consistent with the experiments. Since the size of the structure is less than L_T and L_ϕ , the system is phase coherent.

Figure 2(a) shows the calculated $I-V_D$ curve. We can see that there are many current peaks in this curve. When the well depth V_D increases, the quantum energy level in the well passes through the Fermi energy level of the ring. When one quantum energy level just passes through the Fermi level, resonant transport occurs, which corresponds to a current peak. This can be easily understood. Figures 2(b) and 2(c) demonstrate the relation between the transport current and the magnetic flux through the ring. The phase characteristics at each side of one current peak are clearly shown in the $I-V_D$ curve. Between the two sides of a resonant peak, the phase changes by π . This is in accordance with the usual case when an AB ring is connected to two normal metals. In our case, the total transport current is the sum of the electron and hole contributions. Although electrons and holes have different charge and energy, they have the same phase change when resonant transport occurs. Therefore, the total transport current has a phase change π across the peak as if there are only electrons in the system.

From Figs. 2(b) and 2(c) we can see that the current peaks appear periodically but their values decrease with increasing threading magnetic flux. This ‘‘quasiperiodic’’ phenomenon is different from the case when an AB ring is placed between two normal metals (there all peaks have the same value). This can be understood by considering the fact that electrons and holes have contrasting additional phases when they move in the same direction in the AB ring. In our case, the magnetic flux affects not only the phases of electrons but also their wave vectors. With increasing magnetic flux, the difference between the wave vector of the electron and the wave vector of the hole increases. Some of the electrons are induced by Andreev reflection of holes, and have the same wave vector as the holes [see Eq. (1)]. With increasing magnetic flux, the difference between the wave vectors of electrons increases, which weakens the coupling between electrons. So the total current decreases. In Fig. 3, we show $I-\Phi$

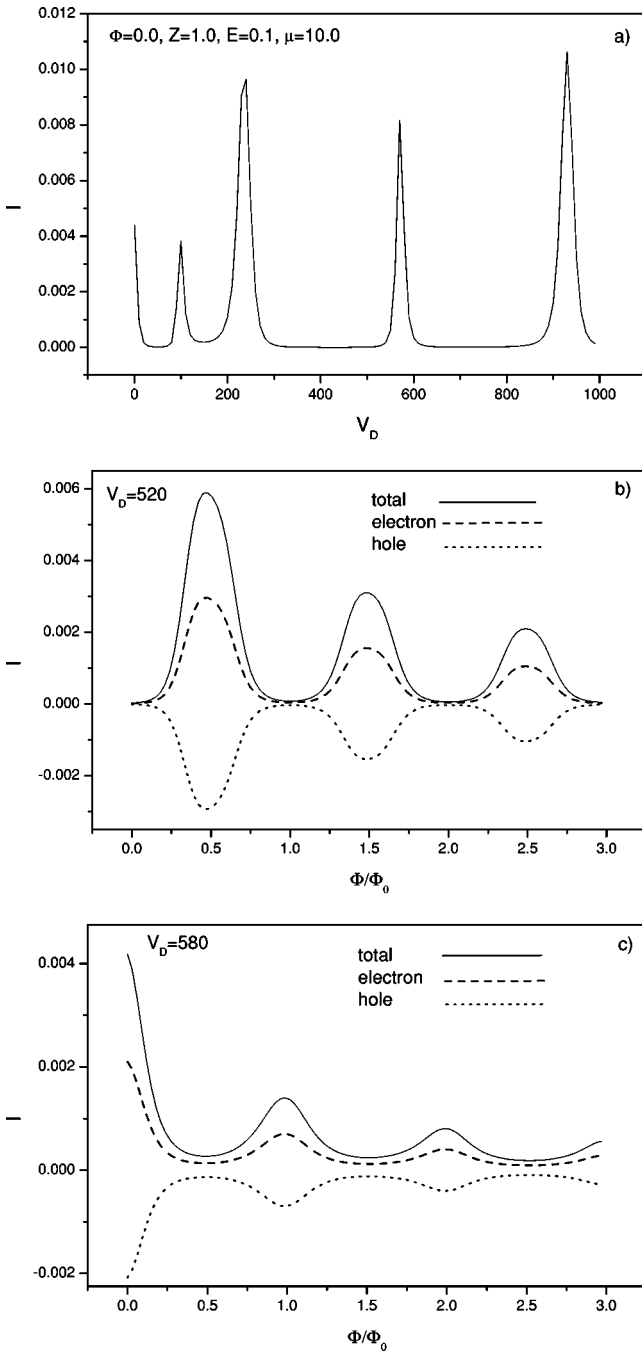


FIG. 2. The total transport current I versus dot potential V_D (a), and the transport current I versus Φ for $V_D=520$ (b) and $V_D=580$ (c). Here we choose $Z=1.0$, $E=0.1$, and $\mu=10.0$. Φ is taken to be zero for (a).

curves for the usual ring structure connected to normal conductors and for the structure that is connected to the superconductor and normal conductor. We can see that, when only electrons contribute to the transport current, the current is a ‘‘standard’’ periodic function of the magnetic flux, with a period equal to the flux quantum Φ_0 . Obviously, it is the superconductor that results in the above-mentioned quasiperiodic behavior of the transport current. This result might be verified by an experiment with this system under a low magnetic field.

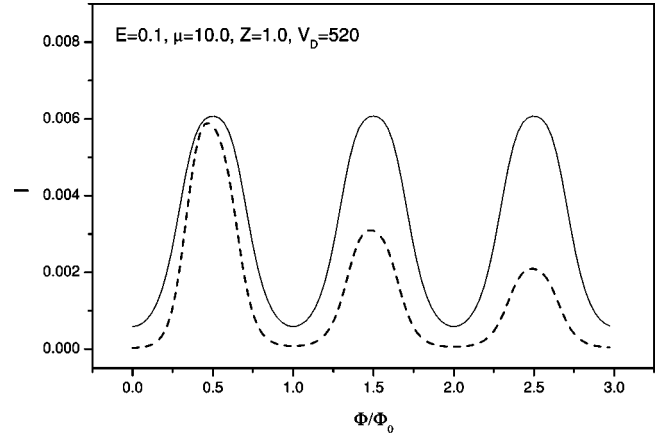


FIG. 3. The total transport current I versus magnetic flux Φ for our proposed structure with a superconductor as shown in Fig. 1(a) (dashed line) and the usual structure without a superconductor (solid line).

Finally, we study the relation between the transport current and the lead l_5 that connects the AB ring to the superconductor. We observe a significant dependence of the transport current on the lead length. Figure 4 shows the transport current I as a function of $k_e L_5$, where k_e and L_5 are, respectively, the wave vector of the electron and the length of the lead l_5 . We can see that the transport current is a periodic function of $k_e L_5$. Let us consider an equivalent big ring with circumference $L+2L_5$. The additional phase is equal to $2k_e L_5$ when particles move to the right lead l_5 from the ring and are reflected back to the ring at the NS interface. We can see that the $I-k_e L_5$ curves are sensitive to the well depth V_D . With the QD far from the resonance state, the transmission probability of the particles through the QD is close to zero and the transport current flows almost entirely through one arm of the ring. When resonant tunneling through the dot occurs, the transmission probability through the QD increases greatly and the current flows through both arms of the ring. Because the phase of the particles will change when they pass through the dot, the interference condition changes

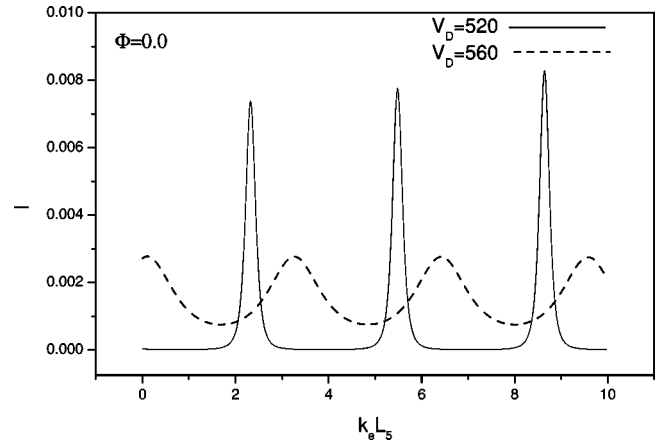


FIG. 4. The total transport current versus the length of the lead l_5 that connects the ring to the superconductor. The parameters are $Z=1.0$, $E=0.1$, $\mu=10.0$, and $\Phi=0.0$.

with varying V_D and consequently the positions of the current peaks in the I - $k_e L_5$ curves are displaced as shown in Fig. 4. Since the length of the lead l_5 is a controllable parameter in the experiment, our result for the dependence of the transport current on the length of the lead could be directly checked by future experiments.

In summary, we have investigated the transport behavior of an AB mesoscopic ring with a QD that differs from the usual systems of this kind in that one of the terminals is connected to a superconductor rather than a normal conductor. In this system, holes are introduced due to Andreev reflection and the total transport current is the sum of electron and hole contributions. The total current has a phase change π when one quantum energy level passes through the Fermi energy level of the system. This can be understood by noting the resonant transport through the dot. We observe that holes

do not influence the phase characteristic of the total current, but they do influence the magnitude of the total current when the magnetic flux varies. We find that the transport current depends significantly on the length of the lead that connects the ring to the superconductor. The reason is that a change of length of the lead affects the wave interference in this system. Our results and conclusions presented above can be checked by future experiments and might provide useful information about the influence of the superconducting proximity effect on the mesoscopic transport properties.

G.Z. would like to acknowledge helpful discussions with Dr. J. Wu and Dr. X. L. Liu. This work was supported by the Natural Science Foundation of China and the Ministry of Science and Technology of China.

*Email address: gzhang@phys.tsinghua.edu.cn

¹A. Yacoby, M. Heiblum, D. Mahalu, and H. Shtrikman, *Phys. Rev. Lett.* **74**, 4047 (1995).

²K. Haule and J. Bonca, *Phys. Rev. B* **59**, 13 087 (1999).

³M. R. Geller, *Phys. Rev. Lett.* **80**, 5393 (1998).

⁴I. V. Zozoulenko, A. S. Sachrajda, C. Gould, K. F. Berggren, P. Zawadzki, Y. Feng, and Z. Wasilewski, *Phys. Rev. Lett.* **83**, 1838 (1999).

⁵V. Ferrari, G. Chiappe, E. V. Anda, and M. A. Davidovich, *Phys. Rev. Lett.* **82**, 5088 (1999).

⁶K. Kang, *Phys. Rev. B* **59**, 4608 (1999).

⁷A. Leay Yeyati and M. Büttiker, *Phys. Rev. B* **52**, R14 360 (1995).

⁸G. Hackenbroich and H. A. Weidenmuller, *Phys. Rev. B* **53**, 16 379 (1996).

⁹G. Hackenbroich and H. A. Weidenmuller, *Phys. Rev. Lett.* **76**, 110 (1996).

¹⁰J. Wu, B. L. Gu, H. Chen, W. Duan, and Y. Kawazoe, *Phys. Rev. Lett.* **80**, 1952 (1998).

¹¹M. Büttiker, *Phys. Rev. Lett.* **57**, 1761 (1986).

¹²R. Schuster and E. Buks, *Nature (London)* **385**, 417 (1997).

¹³A. F. Andreev, *Zh. Éksp. Teor. Fiz.* **46**, 1823 (1964) [*Sov. Phys. JETP* **19**, 1228 (1964)].

¹⁴G. E. Blonder, M. Tinkham, and T. M. Klapwijk, *Phys. Rev. B* **25**, 4515 (1982).

¹⁵M. Octavio, M. Tinkham, G. E. Blonder, and T. M. Klapwijk, *Phys. Rev. B* **27**, 6739 (1983).

¹⁶K. Flensberg, J. B. Hansen, and M. Octavio, *Phys. Rev. B* **38**, 8707 (1988).

¹⁷J. J. Quinn and R. A. Ferrell, *Phys. Rev.* **112**, 812 (1958).

¹⁸I. Campillo, J. M. Pitarke, A. Rubio, E. Zarate, and P. M. Echenique, *Phys. Rev. Lett.* **83**, 2230 (1999).

¹⁹I. Campillo, A. Rubio, J. M. Pitarke, A. Goldmann, and P. M. Echenique, *Phys. Rev. Lett.* **85**, 3241 (2000).

²⁰N. W. Ashcroft and N. D. Mermin, *Solid State Physics* (Holt, Rinehart and Winston, New York, 1976).

²¹P. G. N. de Vegvar, T. A. Fulton, W. H. Mallison, and R. E. Miller, *Phys. Rev. Lett.* **73**, 1416 (1994).

²²Z. Cao, X. P. Yu, and R. S. Han, *J. Phys.: Condens. Matter* **10**, 17 (1998).

²³J. B. Xia, *Phys. Rev. B* **45**, 3593 (1992).